Dissipative solitons under the action of the third-order dispersion

Boris A. Malomed,[1,*] Dimitri J. Frantzeskakis,[2] Hector E. Nistazakis,[2] Andreas Tsigopoulos,[3] and Kyriakos Hizanidis[4]
[1]*Department of Interdisciplinary Studies, Faculty of Engineering, Tel Aviv University, Tel Aviv 69978, Israel*
[2]*Department of Physics, University of Athens, Panepistimiopolis, 157 84 Athens, Greece*
[3]*Department of Electronics, Hellenic Naval Academy, Hatzikyriakou Av., 185 39 Piraeus, Greece*
[4]*Department of Electrical and Computer Engineering, National Technical University of Athens, 9 Iroon Polytechniou, Zografou, 157 73 Athens, Greece*

(Received 5 October 1998; revised manuscript received 3 June 1999)

We study the evolution of a solitary pulse in the cubic complex Ginzburg-Landau equation, including the third-order dispersion (TOD) as a small perturbation. We develop analytical approximations, which yield a TOD-induced velocity c of the pulse as a function of the ratio D of the second-order dispersion and filtering coefficients. The analytical predictions show agreement with the direct numerical simulations for two dinstict intervals of D. A new feature of the pulse motion, which is a precursor of the transition to blowup, is presented: The pulse suddenly acquires a large acceleration in the reverse direction at $D>D_{\rm cr}\approx -1.5$ and without the reversal at $D<D_{\rm cr}$. It is also demonstrated that the laminar-propagation distance L (before the onset of the ultimate turbulent stage) becomes maximum deep inside the normal-dispersion region, while TOD significantly increases L in the anomalous-dispersion region, where, otherwise, it is quite small. The model has a straightforward physical realization in terms of nonlinear optical fibers with losses and bandwidth-limited amplification (gain and filtering). [S1063-651X(99)07709-0]

PACS number(s): 42.81.Dp, 41.20.Jb, 42.81.Wg

I. INTRODUCTION AND FORMULATION OF THE MODEL

As is commonly known, the existence and stability of solitons (which we realize here simply as localized pulses) in various physical systems is provided by the balance between the second-order dispersion (SOD) and nonlinear self-focusing. In many cases, and especially in such an important application as the temporal and spatial solitons in nonlinear optics [1], the nonlinearity is weak, therefore, the solitons cannot be generated unless one is using a carrier wavelength close to the zero-dispersion point (ZDP), where SOD is weak too. In this case, however, two other linear effects may become conspicuous, viz., the third-order dispersion (TOD) and filtering (dispersive losses). TOD is always present in any physical system, and there is no reason to expect that it would vanish at ZDP, where the SOD coefficient vanishes. The natural filtering, existing due to the fact that the loss-compensating amplification is always *bandwidth limited*, can be enhanced by the narrow-passband filters, that are usually inserted into the long fiber link in order to suppress the soliton jitter [2]. In other physical systems where the solitary pulses are observed, dispersive losses also appear naturally; for instance, in the traveling-wave convection in binary fluids, an experimentally measured coefficient of the dispersive losses (diffusivity) is known to be essentially larger than the SOD coefficient [3].

The situation in which the terms accounting for both filtering and TOD may be regarded as small perturbations added to the nonlinear Schrödinger (NLS) equation was studied in detail in terms of the soliton propagation in nonlinear optical fibers [4,5]. In particular, a ''two-stage'' perturbation theory, developed in Ref. [5], produced very accurate results as compared to direct simulations. At the first stage, this version of the perturbation theory took into regard a soliton's phase structure generated by TOD and, at the second stage, the balance equation for the momentum of the soliton was used to calculate its stationary frequency shift induced jointly by TOD and the bandwidth-limited gain.

The objective of the present work is to study the effect produced by the weak TOD in a broad physically relevant region of the parameters, where filtering is not a small perturbation. In the notation adopted for the optical fibers [1], the corresponding general model is

$$iu_z+\left(\frac{1}{2}D-i\right)u_{\tau\tau}+|u|^2u-iu=i\varepsilon u_{\tau\tau\tau}, \qquad (1)$$

where $u(z,\tau)$ is the amplitude of the electromagnetic wave, z and τ are the propagation distance and the so-called reduced time, D is the ratio of SOD and filtering coefficients (the latter one is normalized, as well as the gain and nonlinear coefficients, to be $\equiv 1$), and ε is the relative TOD coefficient. Thus, the model has two dimensionless control parameters: ε, which can always be defined to be positive, and D, whose positive and negative values are nonequivalent, corresponding, respectively, to the *anomalous* and *normal* SOD [1]. Note that, following the generally adopted assumption, Eq. (1) treats the amplification and filtering in the distributed approximation. Nonlinear losses can also be added to the model, but in both physical applications for which the model is well established, viz., the optical fibers and traveling-wave convection, the nonlinear losses are usually negligible.

To estimate relevant values of the control parameters, we recall that the gain bandwidth of the Er-doped optical amplifiers is $\Delta\omega\sim 1$ THz [6], which can be easily reduced by means of filters down to $\Delta\omega\sim 100$ GHz and further. With

*Electronic address: malomed@eng.tau.ac.il

regard to the normal value $\gamma \approx 0.05\,\mathrm{km}^{-1}$ (tantamount to 0.2 dB/km) of the fiber loss to be compensated by the amplification [1], we conclude that the unrenormalized filtering coefficient, $\Gamma \sim \gamma/(\Delta\omega)^2$, can readily take any value from the interval 0.05–5 ps^2/km. As for the unrenormalized SOD coefficient β_2, in the standard telecommunication fibers, $|\beta_2| = 20\,\mathrm{ps}^2/\mathrm{km}$ [1]. Thus, $D = \beta_2/\Gamma$ takes values from the broad interval $|D| \leqslant 400$.

An expression for the dimensionless TOD coefficient ε in Eq. (1) is, in terms of the physical parameters, $\varepsilon = (1/6)\beta_3/\Gamma^{3/2}$, where β_3 is the standard (unrenormalized) TOD coefficients, and Γ is the above-mentioned filtering coefficient. A typical value of the TOD coefficient in the standard telecommunication fiber is $|\beta_3| \leqslant 0.1\,\mathrm{ps}^3/\mathrm{km}$, but it may be made much smaller in the so-called dispersion-flattened fibers [1]. In this work, most numerical results at moderate values of $|D|(|D| \sim 1)$ will be presented for $\varepsilon \sim 10^{-3}$, which corresponds to $\Gamma \sim 5\,\mathrm{ps}^2/\mathrm{km}$ (i.e., relatively strong filtering, that provides for more stable pulse transmission in the standard telecommunication fiber link), or to the dispersion-flattened fibers. Larger values of ε, in combination with $|D| \sim 1$, give rise to very complex dynamics, because of which they are less relevant for the applications. This case may be, nevertheless, interesting by itself, and will be considered in detail elsewhere (nevertheless, we display some essential results, viz., the stable-propagation distance vs D, for $\varepsilon \sim 10^{-2}$ too). In contrast with this, at sufficiently large negative D (deep inside the normal-dispersion region) the pulse propagation turns out to be very robust, irrespective of the smallness of ε, and is amenable to analytical treatment (see Sec. III below). Actually, this case is most promising for the applications to the optical telecommunications [7].

In the case $\varepsilon = 0$, when Eq. (1) is the well-known complex Ginzburg-Landau (CGL) equation, the pulse (dissipative soliton) is described by the well-known exact solution [6],

$$u_0 = A_0 e^{ikz}[\mathrm{sech}(\kappa\tau)]^{1+i\mu}, \tag{2}$$

$$\kappa^2 = 3(1+\mu^2)^{-1}, \quad A_0^2 = \mu^{-1}(4+\mu^2), \quad k = \tfrac{1}{2}D\kappa^2, \tag{3a}$$

the pulse's *chirp* being

$$\mu = \sqrt{\tfrac{9}{16}D^2 + 2} - \tfrac{3}{4}D. \tag{3b}$$

The first objective of this work is to find the soliton's velocity generated by the small TOD term. A natural approach to this is to use the exact solution (3) as the zeroth-order approximation and develop the perturbation theory around it. However, a complete analysis of Eq. (1) linearized around the solution (3), which is the basis for the formal perturbation theory, is a cumbersome mathematical problem. In this work, we are able to find an approximate analytical solution for the velocity (corroborated by direct simulations) in two cases. In Sec. II, we develop a direct perturbation theory, splitting the TOD-induced perturbation into two terms. The first term is tantamount to a complex group-velocity shift, which allows us to obtain an *exact* result produced by this term at the first order of the perturbation theory (at ZDP, $D = 0$, this yields an exact *full* value of the velocity in a very simple form: $c = \varepsilon$). An effect produced by the remaining (second) term in the TOD-induced perturbation is found by means of the momentum-balance equation, i.e., essentially the same way as it was done for the perturbed NLS solitons in [5]. Formally, the momentum balance can be applied when the parameter D is positive and large enough (when the contributions from both perturbation terms turn out to be comparable). However, the relative contribution of the second term, as compared to the exactly found velocity produced by the first one, vanishes $\sim D$ as $D \to 0$. Thanks to this circumstance, the combination of the two terms yields an analytical approximation that is found to be in a fairly reasonable agreement with the numerical results not only at all the values $D \geqslant 0$, but also at negative D up to $D = -1.5$.

In Sec. III we develop another analytical approximation for the case when D is negative and large. In this case, the unperturbed pulse (2) is very broad, which suggests applying the so-called geometric-optics (GO) (or eikonal) approximation, based on the assumption that the local amplitude, wave number, and frequency of the wave field are slowly varying functions. This technique, developed in an earlier work [8], was recently used to successfully predict the velocity of the so-called dark shock wave in a simpler version of the CGL equation [9]. We demonstrate that, in this case, the soliton's velocity takes a limit *constant* value, $c = (\frac{1}{3})\varepsilon$, which is found to be in very good agreement with the numerical results for $D \leqslant -30$.

In Sec. IV, we present results of systematic numerical simulations of the model. Comparing the numerically found dependence $c(D)$ with the two above-mentioned analytical predictions, we find the agreement, as was already mentioned above, in two regions, $D \leqslant -30$ and $D > -1.5$. In the gap between them, neither approximation applies, and there we find novel features in the dependence $c(D)$, viz., a very steep downjump, with a change of the sign of c, at $D = D_{\mathrm{cr}} \approx -1.5$, and a smoother transition in the opposite direction at $-30 < D < -20$ (see Fig. 4 below).

As well as the CGL equation, the model (1) is inherently unstable, as it contains the linear-gain term. This instability is a well-known drawback of the exact solution (2), which, however, did not impede its successful use in various contexts. The instability demonstrates itself in the form of a blowup that switches the system into a turbulent state. However, the blowup follows a relatively long period of regular (''laminar'') evolution of the pulse [which makes it possible to measure numerically the dependence $c(D)$]. Moreover, in particular physical applications the blowup can be prevented by various means (e.g., circulating an optical pulse in a fiber loop [10], or, in the case of the traveling-wave convection [3], taking into regard the fact that, in the real experiment, the pulse is circulating in an annulus [11]). In any case, for the applications it is very important to know not only the dependence $c(D)$, but also the laminar-propagation distance L as a function of D. This dependence is also displayed in Sec. IV, showing that L is much larger for sufficiently large negative D than at its other values. The latter result lends more value to the above-mentioned analytical prediction of the asymptotic velocity, $c = \frac{1}{3}\varepsilon$, valid in the same region. As for the influence of TOD, we find that it is significant at $D \geqslant 3$, making L larger (which is, otherwise, quite small in this case). Additionally, we find a new feature, viz., a *precursor*

of the blowup, in the form of sudden acceleration or deceleration of the moving pulse at the last stage of its laminar evolution.

In Sec. IV, we also briefly consider a modified model, with *sliding-frequency* filtering, which is a well-known means for suppression of the soliton's jitter in the fiber communication lines [12]. The simulations demonstrate that the frequency sliding slightly increases the laminar-propagation distance.

II. PERTURBATION THEORY FOR THE PULSE

It is well known that, in the absence of filtering, the effect of TOD on the NLS soliton can be analyzed by means of the perturbation theory [13]. Here, our aim is to develop a perturbative treatment of TOD acting on the CGL pulse (2).

Treating the TOD term on the right-hand side of Eq. (1) in the first order of the perturbation theory, we substitute the expression (2) into it, and notice that exactly the same perturbation would be produced, at the first order, by the following effective perturbation replacing the right-hand side of Eq. (1):

$$P_{\rm eff}=-icu_\tau+id|u|^2u_\tau, \tag{4}$$

$$\begin{aligned} c&\equiv-3\varepsilon(1+i\mu)^2(1+\mu^2)^{-1},\\ d&\equiv-3\varepsilon\mu(3+i\mu)(1+\mu^2)^{-1}(2-i\mu)^{-1}. \end{aligned} \tag{5}$$

The effect of the first effective perturbation term, which is nothing else but a complex group velocity, can be taken into account in an obvious way: one first makes the substitution $u\equiv\tilde{u}\exp(-i\omega\tau)$, with $\omega=-\frac{1}{2}\,{\rm Im}\,c$, which eliminates the imaginary part of the complex group velocity c, and, through the SOD term, simultaneously gives rise to an additional contribution to the real part of c, $\Delta({\rm Re}\,c)=-D\omega\equiv\frac{1}{2}D\,{\rm Im}\,c$. Finally, the remaining net real part of c implies that sech$(\kappa\tau)$ in the solitary-pulse solution (2) should be replaced by sech$[\kappa(\tau-c_1z)]$ with the effective velocity $c_1={\rm Re}\,c+\frac{1}{2}D\,{\rm Im}\,c$. Using the above expressions, the latter result can be cast into the following form:

$$\frac{c_1}{\varepsilon}=\frac{1+\frac{15}{8}D^2-\frac{5}{2}D\sqrt{\frac{9}{16}D^2+2}}{1+\frac{3}{8}D^2-\frac{1}{2}D\sqrt{\frac{9}{16}D^2+2}}. \tag{6}$$

The second term in Eq. (4) cannot be treated in an exact way, unlike what was done above with the first term. In this case, the only straightforward approach can be based on the balance equation for the soliton's momentum, $M=-i\int_{-\infty}^{+\infty}uu_\tau^*d\tau$, where the asterisk stands for the complex conjugation. The balance implies vanishing of the net sum of the *forces*, i.e., contributions to dM/dz, generated by the gain and filtering terms in Eq. (1) and the second perturbation term in Eq. (4), for the soliton moving at some velocity c_2. The calculations can be easily performed, following the lines of Ref. [5], which yields an additional contribution to the velocity, cf. Eq. (6):

$$\frac{c_2}{\varepsilon}=\frac{D\sqrt{\frac{9}{16}D^2+2}-\frac{3}{4}D^2}{1+\frac{3}{8}D^2-\frac{1}{2}D\sqrt{\frac{9}{16}D^2+2}}. \tag{7}$$

Finally, adding up the expressions (6) and (7), we arrive at an eventual analytical prediction for the soliton's velocity provided by the perturbation theory:

$$\frac{c}{\varepsilon}=\frac{1+\frac{9}{8}D^2-\frac{3}{2}D\sqrt{\frac{9}{16}D^2+2}}{1+\frac{3}{8}D^2-\frac{1}{2}D\sqrt{\frac{9}{16}D^2+2}}. \tag{8}$$

Note that, according to this expression, c vanishes at $D=\frac{2}{3}$, and $c/\varepsilon=1$ at $D=0$. The latter result is *exact*, as the second perturbation term in Eq. (4), that cannot be treated exactly, vanishes at $D=0$.

One should bear in mind that the applicability of the momentum-balance equation is, strictly speaking, limited to the case of sufficiently large positive values of D, when the pulse (2) is close to the NLS soliton, and the filtering term in Eq. (1) is small as compared to the dispersion, otherwise the equation does not approximately conserve the momentum even at the zero order, $\varepsilon=0$. Nevertheless, the comparison of the analytical prediction for $c(D)$ given by Eq. (8) with the direct simulations (see Sec. IV) will show good agreement at $D>-1.5$. The agreement can be easily explained: with the decrease of D from large positive values, where the approximation must work automatically, the contribution (7) from the second term in the effective perturbation (4) indeed becomes inaccurate, but it decreases $\sim D$, while the dominant (nonvanishing) contribution (6) from the first term is *exact*.

III. GEOMETRIC-OPTICS APPROXIMATION

The GO approximation can be applied to fields with slowly varying local amplitude, wave number, and frequency [8]. As it follows from the form of the exact unperturbed pulse solution (2) and (3), a natural case for this is $-D\gg1$, when the pulse is broad, its width being $\sim\kappa^{-1}\approx(\sqrt{3}/2)|D|$.

We start from the representation of the complex field in the form

$$u(z,\tau)=\alpha(z,\tau)\exp[i\varphi(z,\tau)], \tag{9}$$

where α and φ are the real amplitude and phase. Insertion of Eq. (9) into Eq. (1) leads to coupled real equations for α and φ that have a rather cumbersome form. To simplify them, we now resort to the GO approximation, which assumes that the amplitude α and the local wave number φ_z and frequency $-\varphi_\tau$ are slowly varying functions of τ, so that their τ derivatives are small quantities. However, to be consistently implemented, this approximation needs a large parameter in Eq. (1). It will be seen below that the necessary large parameter is $-D$.

It is easy to see that the first real equation obtained by the substitution of Eq. (9) into Eq. (1), viz., the evolution equation for the phase, contains terms of the zero order with respect to the GO smallness. Keeping only these terms, we obtain the first simplified equation in the form

$$\alpha^2=\varphi_z+\frac{1}{2}D\varphi_\tau^2+\varepsilon\varphi_\tau^3. \tag{10}$$

The second equation, which governs the evolution of the amplitude, contains the zero-order terms, and, in addition to them, several terms of the first order which are multiplied by

the large parameter D. It will be verified below that the self-consistent approximation implies that the large $|D|$ compensates the first-order GO smallness. With regard to this, the second equation (multiplied by 2α) can be written in the form

$$2\alpha\alpha_z + D(\alpha^2\varphi_{\tau\tau} + 2\alpha\alpha_\tau\varphi_\tau) + 6\varepsilon\alpha\alpha_\tau\varphi_\tau^2 + 6\varepsilon\alpha^2\varphi_\tau\varphi_{\tau\tau} = 2\alpha^3 - 2\alpha^2\varphi_\tau^2. \tag{11}$$

The terms $\sim\varepsilon$ are kept in this equation [as well as in Eq. (10)] as a small correction that will later give rise to the soliton's velocity. To summarize, the terms omitted when deriving the simplified equations (10) and (11) from Eq. (1) are those containing the first- and second-order GO smallness in the filtering term on the right-hand side of Eq. (1), and the second- and third-order smallness in the third-dispersion term.

A solution to Eqs. (10) and (11) that describes a traveling soliton is looked for as

$$\alpha = \alpha(\tau - cz), \quad \varphi = kz + \psi(\tau - cz), \tag{12}$$

where k is a constant. Then, in terms of

$$p \equiv d\psi/d\xi, \quad \xi \equiv \tau - cz, \tag{13}$$

Eq. (10) transforms into a simple algebraic relation,

$$\alpha^2 = \varphi_z + \tfrac{1}{2}D\varphi_\tau^2 + \varepsilon\varphi_\tau^3. \tag{14}$$

Substituting Eq. (13) into Eq. (11), we make use of a relation obtained by the differentiation of Eq. (14),

$$d(\alpha^2)/d\xi = (Dp - c + 3\varepsilon p^2)(dp/d\xi). \tag{15}$$

One should also recall that ε is an independent small parameter, and the velocity c sought for is expected to be $\sim\varepsilon$, hence it has the same smallness as ε. Making use of Eq. (15), and omitting the second-order terms $\sim c^2$, ε^2, and $c\varepsilon$, we finally cast Eq. (11) into the form

$$\left[D\left(\frac{3}{2}Dp^2 + k\right) - 3cDp + 10\varepsilon Dp^3 + 6\varepsilon kp\right]\frac{dp}{d\xi} = 2(1-p^2)\left(k - cp + \frac{1}{2}Dp^2 + \varepsilon p^3\right). \tag{16}$$

This is a ''master equation'' in the present case, $-D \gg 1$.

A soliton solution is singled out by the obvious boundary conditions, $\alpha(\xi = \pm\infty) = 0$. As it follows from Eq. (14), the variable $p(\xi)$, which is governed by Eq. (16), must take, at $\xi = \pm\infty$, constant values p_0 which nullify the right-hand side of Eq. (14). Thus, Eq. (16) must be complemented by the boundary conditions $dp/d\xi = 0$ at $\xi = \pm\infty$. As concerns the constants k and c, they are, as a matter of fact, unknown *eigenvalues* that must be found as a part of the solution.

First, we consider the zero-order approximation in ε, setting $\varepsilon = c = 0$. In this case, Eq. (16) further simplifies:

$$(3Dp^2 + 2k)\frac{dp}{d\xi} = \frac{2}{D}(1-p^2)(2k + Dp^2), \tag{17}$$

and the values of p providing for $\alpha^2 = 0$ are, according to Eq. (14),

$$p_0 = \pm\sqrt{-2k/D}. \tag{18}$$

Because Eq. (17) is the first-order ordinary differential equation, its only possible nontrivial solution with the asymptotic values (18) at $\xi = \pm\infty$ is an antisymmetric $[p(-\xi) = p(\xi)]$ kink, which takes all the values from the interval

$$|p(\xi)| \leqslant \sqrt{-2k/D}. \tag{19}$$

Here, however, we encounter a problem, because, inside the interval (19), there are two values $p = \pm\sqrt{-2k/3D}$, at which the denominator of the right-hand side of Eq. (17) vanishes, hence the solution will be singular. Indeed, straightforward integration of Eq. (17) shows that, in a vicinity of a point ξ_0 at which $p = \pm\sqrt{-2k/3D}$, the form of the solution is

$$(p \mp \sqrt{-2k/3D})^2 \approx \mp(2/3D)^2\sqrt{-2k/3D}(3D + 2k)(\xi - \xi_0). \tag{20}$$

As it follows from Eq. (20), the only way to avoid the singularity is to set

$$k = -\tfrac{3}{2}D, \tag{21}$$

which yields the unknown eigenvalue in the present approximation. From the viewpoint of Eq. (17), this implies that the expression multiplying $dp/d\xi$ vanishes at the same point, $p^2 = 1$, at which the multiplier $(1 - p^2)$ on the right-hand side vanishes. It then follows from Eq. (18) that the asymptotic wave numbers are $p_0^2 = 3$.

In the next approximation, we demand that, in the first order with respect to the small parameters ε and c, the same mechanism of canceling the singularity holds in Eq. (16), i.e., the expression multiplying $dp/d\xi$ must vanish at $p^2 = 1$. A straightforward calculation yields

$$c/\varepsilon = 1/3. \tag{22}$$

This is the eventual (and fairly simple) analytical result predicting the soliton's velocity for $-D \gg 1$.

IV. NUMERICAL RESULTS AND THEIR INTERPRETATION

We performed systematic simulations of the CGL equation (1) with small values of the TOD parameter ε. Most results displayed below pertain to $\varepsilon = 10^{-3}$, which, as was explained in the Introduction, is the value of practical interest for small D and $|D| \sim 1$. Some essential results are also presented for $\varepsilon = 10^{-2}$. However, detailed results for ε essentially larger than 10^{-3} are not reported here in this region of the values of $|D|$, as they are very complex (hence, they are less interesting for the applications), and will be presented elsewhere. On the contrary to this, the results for sufficiently large negative D, when the pulse turns out to be very robust, turn out to be essentially the same for all reasonably small ε (e.g., $\varepsilon = 10^{-2}$ and $\varepsilon = 10^{-1}$). These results,

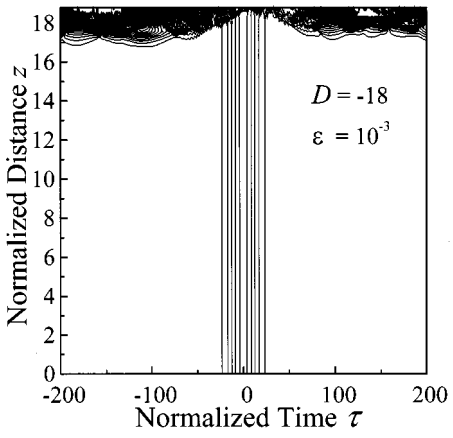

FIG. 1. An example of the evolution of the pulse in the model (1) at $D=-18$ and $\varepsilon=10^{-3}$, ending up with the onset of the ''turbulence'' via the blowup.

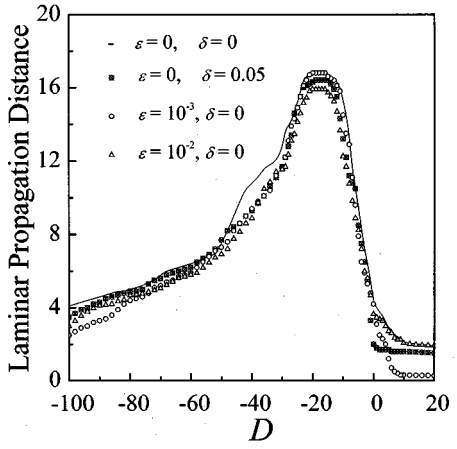

FIG. 2. The laminar-propagation distance, defined as 80% of the distance at which the blowup takes place, vs D. The continuous curve corresponds to the case $\varepsilon=0$, $\delta=0$, while the three different dotted curves correspond to the following cases: $\varepsilon=0$, $\delta=0.05$; $\varepsilon=10^{-2}$, $\delta=0$, and $\varepsilon=10^{-3}$, $\delta=0$ [recall δ is the frequency-sliding slope in the modified model (23)].

which may also be of considerable interest for the applications to the optical-fiber communications, are displayed below.

As the initial configuration, we always took the exact pulse solution given by Eqs. (2)–(4). The simulations were run on the basis of a finite-difference scheme in a wide interval of the variable τ, that was always chosen to be much larger than the pulse's width. In order to prevent the possible radiation emitted by the pulse from reappearing in the integration domain, we used a standard device, placing narrow strongly absorbing layers at the edges of the domain.

Because the linear-gain term makes the model intrinsically unstable, the evolution always ends with a transition to a turbulentlike behavior through blowup. An example is displayed in Fig. 1 for $\varepsilon=10^{-3}$ and $D=-18$. In this example, the blowup starts at the very end of the simulated propagation distance. Actually, at this value of D, the laminar-propagation distance attains its maximum and is nearly independent of ε, as will be discussed below.

In addition to the model (1), we have also considered a modified model, with the usual (*fixed-frequency*) filtering replaced by the *sliding-frequency* filtering [12], which is a popular means for suppression of the *Gordon-Haus jitter* of the soliton, induced by its interaction with the radiation spontaneously emitted by the amplifiers. In view of the considerable practical importance of the frequency sliding, it is quite relevant to investigate its impact on the soliton dynamics in the present model. To this end, Eq. (1) was modified as follows [12]:

$$iu_z+(\tfrac{1}{2}D-i)u_{\tau\tau}+|u|^2u-iu=i\varepsilon u_{\tau\tau\tau}+2i\Omega_F u_\tau-i\Omega_F^2 u, \tag{23}$$

where $\Omega_F\equiv\Omega_F(z)$ is the sliding frequency, which is assumed to be a linear function of z, $\Omega_F(z)=\delta z$, with a real slope constant δ.

A systematic study of basic features of the pulse's evolution before the blowup reveals a number of nontrivial features that are summarized below. In the application to the optical fibers, such finite-propagation-length results are physically meaningful, as the fiber's length in the experiment may be shorter than is necessary for the onset of the blowup, but long enough to observe (and use) nontrivial features in the preblowup dynamics, provided that the laminar-propagation distance essentially exceeds the pulse's *dispersion length*, see below. Moreover, as was mentioned in the Introduction, in real physical systems the model can be modified by means of the boundary conditions, so that the blowup will not take place at all (e.g., in the fiber loop).

The numerically observed features reported below were collected from the propagation distances taken as 80% of the blowup-onset distance, in order to exclude the influence of possible irregularities starting shortly before the onset. In this connection, it is first of all interesting to display the data showing this 80% distance vs both control parameters of the model, D and ε. In Fig. 2, the data are shown for $\varepsilon=10^{-3}$ and 10^{-2}. These plots reveal noteworthy peculiarities: the solitary pulse remains stable much longer if the dispersion is *normal*, $D<0$, than when it is *anomalous*, $D>0$, and, on the other hand, an almost flat maximum of the laminar-propagation distance is observed around $D=-18$. This means that, on the contrary to what is commonly assumed, the best long-distance optical-pulse transmission may be achieved in the *normal-dispersion* regime.

The strong stabilization observed at large negative D can be qualitatively explained. The explanation given below is related to the ''perturbation-sweeping'' mechanism that explains, for the CGL equation with the periodic boundary conditions, an effective stability of the circulating pulse in a parametric region where it was expected to be unstable [11] (see also [14]).

We start the explanation by noting that the linearization of Eq. (1) yields the inverse group velocity $C(\omega)=-D\omega$ for a linear radiation mode with the frequency ω and amplitude $A_1, u_1\sim A_1\exp(-i\omega\tau)$ (here, we neglect a small contribution from TOD). This means that, at large $|D|$, the most danger-

ous destabilizing perturbations are those with a small frequency ω, as, otherwise, the perturbation quickly traverses the integration domain (including its part occupied by the pulse), and is then absorbed at the edges. Besides that, the damping by the filtering term is negligible for the low-frequency perturbation.

On the other hand, due to the presence of the self-focusing cubic term, a low-frequency *slowly moving* perturbation can be (temporarily) captured by the pulse (2) with the large amplitude $A_0 \approx \sqrt{\frac{3}{2}|D|}$ when the perturbation hits the pulse (note that, in a real optical communication line, one is dealing with a quasiperiodic chain of the pulses, hence the absorbing boundary conditions replace, as a matter of fact, the interaction of the radiation with the next pulse). As a result of the interaction with the pulse (u_0), the low-frequency perturbation u_1 generates, through the four-wave mixing induced by the cubic term, a conjugate wave component $\tilde{u}_1 \sim u_0^2 u_1^*$. According to Eqs. (2) and (3), the conjugate component has a *nonsmall* frequency $\Omega \sim 2\kappa\mu \approx 2\sqrt{3}$, and an enhanced amplitude $\tilde{A}_1 \sim A_0^2 A_1$. These, in turn, give rise to strong damping of the perturbation by the filtering term, despite the circumstance that, for the original small frequency ω, the filtering effect is negligible. Even if we do not take into regard the above-mentioned fact that the perturbation may be temporarily captured inside the pulse, the enhanced amplitude and nonsmall frequency of the conjugate component predict the following estimate for the ratio of the stabilizing *effective* average filtering coefficient $\tilde{\Gamma}$ to the destabilizing gain coefficient γ:

$$\tilde{\Gamma}/\gamma \sim \Omega^2 A_0^2 (\tau_0/T) \sim 20|D|(\tau_0/T), \tag{24}$$

where τ_0 and T are, respectively, the temporal width of the soliton and the size of the temporal domain (actually, T the temporal separation between adjacent pulses, in the case of the pulse array in a long fiber communication line), and the above expressions for $\tilde{A}_1$ and Ω have been used. The strong stabilization in the case of large negative D is evident in Eq. (24).

The laminar-propagation distance is not especially sensitive to the value of the TOD coefficient in the normal-dispersion region, but Fig. 2 demonstrates a significant *stabilizing effect* of TOD in the region of anomalous dispersion. Note that a conspicuous stabilizing effect of TOD on the propagation of the ''breathing'' (vibrating) pulses in the *dispersion-management* model, i.e., the lossless model with periodically modulated sign-changing SOD coefficient $D(z)$, was discovered in Ref. [15]. Finally, we see in Fig. 2 that (quite naturally) the frequency sliding increases the laminar-propagation distance, but the increase is quite modest.

The simulations also reveal a novel specific feature of the last stage of the laminar evolution, which precedes the blowup: as is seen in Fig. 3 (for $\varepsilon = 10^{-3}$), at the values $D > D_{\rm cr} \approx -1.5$, the pulse, shortly before the onset of the blowup, suddenly stops and then begins to move in the opposite direction, demonstrating a strong acceleration. Sometimes, this happens with intermediate stops and reversals of the direction of motion. At $D < -1.5$, the pulse's motion also

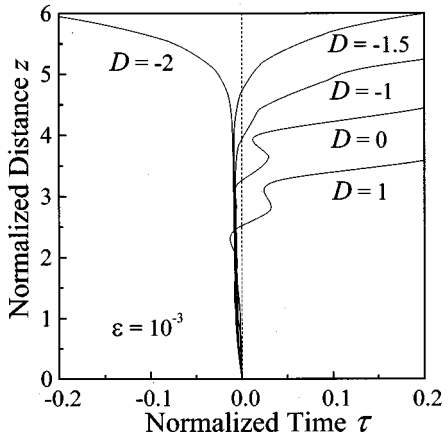

FIG. 3. Trajectories of the pulse motion on the plane (position, propagation distance) for $\varepsilon = 10^{-3}$ and various values of D. The abrupt acceleration of the pulse preceding the blowup is clearly seen.

demonstrates an abrupt acceleration, but this time without the reversal of the original direction of motion. The critical value $D_{\rm cr}$ of D, separating the cases of the reverse and direct acceleration, depends on ε: it shifts farther into the normal-dispersion region with the decrease of ε; for instance, $D_{\rm cr}(\varepsilon = 10^{-4}) \approx -2.0$.

The most essential result describing the soliton's motion at the laminar stage, viz, the soliton's normalized mean velocity c/ε, averaged over the above-mentioned 80% blowup distance, vs the SOD parameter D, is presented in Fig. 4. As is seen in the inset of this plot (corresponding to the case where $-10 \leqslant D \leqslant 10$ and $\varepsilon = 10^{-3}$), there is a very steep jump of the velocity at a critical value $D_{\rm cr}$, which, up to the accuracy of the numerical data, is *the same* as that which separates the reverse and direct accelerations in Fig. 3. To

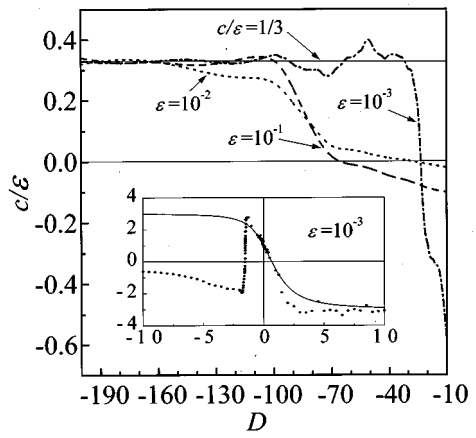

FIG. 4. Numerically found normalized soliton's mean velocity, c/ε, corresponding to the propagation distance equal to 80% of the blowup distance, vs $D(<-10)$ for three different values of ε (10^{-3}, 10^{-2}, and 10^{-1}). The horizontal solid line is the asymptotic value (22) analytically predicted for large negative D. In the inset, the continuous curve shows the analytical prediction given by Eq. (8) for positive and small negative values of D, while the dots are the numerical results obtained for $\varepsilon = 10^{-3}$.

the right of the jump, the numerically found dependence $c(D)$ is quite close to the analytical prediction given by Eq. (8). In particular, in exact accord with the analysis, the numerical and analytically predicted values of the velocity perfectly coincide at the zero-dispersion point $D=0$, both giving $c/\varepsilon=1$.

As was explained in Sec. II, it is natural to expect that the analytical result (8) becomes irrelevant at $D<0$. A surprising fact is that the departure of the numerical results from the analytical prediction occurs relatively late (at $D\approx-1.5$), and so abruptly. More work is necessary to understand a cause for this steep jump.

A less steep transition of the velocity, in the opposite direction, is seen in Fig. 4, for various values of ε (i.e., $\varepsilon=10^{-3}$, 10^{-2}, and 10^{-1}). For example, in the case $\varepsilon=10^{-3}$, this transition takes place between $D=-20$ and -30, and, at $D\leqslant-30$, the observed velocity is very close to the constant value (22), analytically predicted in Sec. III for large negative D. The latter result has an important purport, as the laminar-propagation distance, to which the result (22) pertains, is very large just at large negative D.

Although the accuracy of the analytical prediction (22) is expected to worsen as ε is increased (the asymptotic analysis explicitly assumed ε to be a small parameter), the predicted asymptotic value $c/\varepsilon=1/3$ is reached for $\varepsilon=10^{-2}$ and 10^{-1} as well. However, as is observed in Fig. 4, the region where the prediction is correct gets shifted to the left: This is due to the fact that the larger values of ε may only be compensated (for the applicability of the prediction $c/\varepsilon=1/3$) by better applicability of the GO approximation, which demands a broader pulse, and hence larger negative D.

As was mentioned above, the results obtained for the finite propagation distances are physically meaningful provided that the propagation distance essentially exceeds the *dispersion length* of the pulse (2), which is [1] $z_D\cong\pi/D\kappa^2\mu^2\cong(1+\mu^2)/D\mu$ for the essentially chirped pulses at $D<0$, and $z_D\cong\pi/D\kappa^2\cong(1+\mu^2)/D$ for the unchirped ones at $D>0$ [see Eqs. (2) and (3)]. A few dispersion lengths is the propagation distance necessary for formation of the soliton. Using the data from Fig. 2, we conclude that, for $\varepsilon=10^{-3}$, the ratio of the 80% blowup distance to z_D is very large for $D<-1$, then it is ~10 for $-1<D<5$, and the ratio gets smaller for $D>5$, so that the results are less relevant in the latter region. This consideration demonstrates, once again, the potential of the pulse transmission in the filtered nonlinear optical fibers deep inside the normal-dispersion region.

The velocity also depends on the value of the TOD coefficient ε. In the case $\varepsilon=10^{-4}$, the dependence $c(D)$ for $|D|\leqslant10$ is similar to that for $\varepsilon=10^{-3}$ (see inset of Fig. 4), with the jump shifted to $D_{\rm cr}\cong-2.0$, so that the applicability range for the analytical result (8) slightly expands in this case. However, the numerical results for the velocity at positive and relatively small negative D turn out to be very complex at $\varepsilon=10^{-2}$ (on the contrary to the simple results displayed above for sufficiently large negative D at $\varepsilon=10^{-2}$ and 10^{-1}). Detailed consideration of this case is beyond the framework of the present work.

V. CONCLUSION

In this work, we have studied in detail evolution of the solitary pulse (dissipative soliton) in the complex cubic Ginzburg-Landau equation, which includes the Kerr nonlinearity, linear gain, fixed- or sliding-frequency filtering, and, as a small perturbation, the third-order dispersion, while the second-order dispersion may be anomalous, normal, or zero. Starting from the exact localized-pulse solution to the CGL equation without TOD, we developed a perturbation theory, which treats a part of the effective perturbation generated by TOD in an exact way, while the other part is treated by means of the momentum-balance equation. The analytical prediction for the TOD-induced velocity c was compared to numerical data, showing that the perturbative result is quite accurate in the region of its applicability and beyond, provided the ratio of the second-order dispersion and filtering coefficients D is $\geqslant-1.5$. An alternative analytical approximation, based on the ''geometric-optics'' technique, was developed for large negative D, yielding an asymptotically constant velocity, which is found to be in good agreement with the numerical results for $D\leqslant-30$ (this, and still larger, values of $|D|$ are physically meaningful). In the gap between the two regions of applicability of the analytical approximations, novel features are found in the simulations: at $D\approx-1.5$, the dependence $c(D)$ makes an abrupt jump with the change of its sign, and a smoother transition in the opposite direction takes place at $-30<D<-20$. Numerical simulations also reveal another unexpected feature: before the onset of the ultimate turbulent stage, the pulse suddenly develops a very large acceleration in the reverse direction at $D>-1.5$, and without the direction reversal at $D<-1.5$.

Another set of the numerical results shows the dependence of the preblowup propagation distance L vs the control parameters. The most essential result is that L (both its absolute value and the value normalized to the pulse's dispersion length) is very large for sufficiently large negative D (i.e., deep inside the normal-dispersion region), for which a qualitative explanation is proposed. TOD does not conspicuously affect L in the normal-dispersion region, but stabilizes the propagation (increasing L) at $D>0$. Finally, the frequency-sliding filtering only slightly increases L in comparison with the usual fixed-frequency sliding.

ACKNOWLEDGMENTS

This work has been supported in part by the General Secretariat of Research and Technology of the Hellenic Ministry of Development (PENED-95 Grant Nos. 1242 and 644), and by the Special Research Account of the University of Athens. Constructive discussions with Professor K. Tsakalis (State University of Arizona, Phoenix), Professor D. Reisis (University of Athens, Athens, Greece), and Professor G. Savvidy (Democritos Nuclear Research Center, Athens, Greece) are gratefully appreciated. B. A. M. appreciates the hospitality of the Department of Physics, University of Athens.

[1] G. P. Agrawal, *Nonlinear Fiber Optics* (Academic, San Diego, 1995).

[2] A. Mecozzi, J. D. Moores, H. A. Haus, and Y. Lai, Opt. Lett. **16**, 841 (1991); Y. Kodama and A. Hasegawa, *ibid.* **17**, 31 (1992).

[3] J. A. Glazier, P. Kolodner, and H. Williams, J. Stat. Phys. **64**, 945 (1991).

[4] A. B. Aceves, C. D. Angelis, G. Nalesso, and M. Santagiustina, Opt. Lett. **19**, 2104 (1994); I. M. Uzunov, M. Gölles, and F. Lederer, Phys. Rev. E **52**, 1059 (1995); E. A. Golovchenko, A. N. Pilipetskii, C. R. Menyuk, J. P. Gordon, and L. F. Mollenauer, Opt. Lett. **20**, 539 (1995).

[5] B. A. Malomed, I. M. Uzunov, M. Gölles, and F. Lederer, Phys. Rev. E **55**, 3777 (1997).

[6] E. Desurvire, *Erbium-Doped Fiber Amplifiers* (Wiley, New York, 1994).

[7] N. R. Pereira and L. Stenflo, Phys. Fluids **20**, 1733 (1977); L. M. Hocking and K. Stewartson, Proc. R. Soc. London, Ser. A **326**, 289 (1972).

[8] B. A. Malomed, Physica D **8**, 353 (1983).

[9] A. R. Bishop, D. Cai, N. Gronbech-Jensen, and B. A. Malomed, Phys. Rev. Lett. **78**, 223 (1997).

[10] B. A. Malomed and F. Mitschke, Fiber Integr. Opt. **17**, 267 (1998).

[11] M. van Hecke, E. de Wit, and W. van Saarloos, Phys. Rev. Lett. **75**, 3830 (1995).

[12] M. Desaix, D. Anderson, and M. Lisak, Opt. Lett. **15**, 18 (1990); P. K. A. Wai, H. H. Chen, and Y. C. Lee, Phys. Rev. A **41**, 426 (1990); R. H. J. Grimshaw, Stud. Appl. Math. **94**, 257 (1995).

[13] B. A. Malomed, M. Gölles, I. M. Uzunov, and F. Lederer, Phys. Scr. **55**, 73 (1997).

[14] K. Hizanidis, B. A. Malomed, H. E. Nistazakis, and D. J. Frantzeskakis, Pure Appl. Opt. **7**, L57 (1998).

[15] L. F. Mollenauer, J. P. Gordon, and S. Evangelides, Opt. Lett. **17**, 1575 (1992).